Received: 18 March 2024 | Revised: 1 July 2024 | Accepted: 3 August 2024

DOI: 10.1002/jor.25960

RESEARCH ARTICLE

Journal of Orthopaedic Research®

Degradation of lubricating molecules in synovial fluid alters chondrocyte sensitivity to shear strain

Steven Ayala[1] | **Salman O. Matan**[1] | **Michelle L. Delco**[2] | **Lisa A. Fortier**[2] | **Itai Cohen**[3] | **Lawrence J. Bonassar**[1,4]

[1]Meinig School of Biomedical Engineering, Cornell University, Ithaca, New York, USA

[2]Department of Clinical Sciences, Cornell University College of Veterinary Medicine, Ithaca, New York, USA

[3]Department of Physics, Cornell University, Ithaca, New York, USA

[4]Sibley School of Mechanical and Aerospace Engineering, Cornell University, Ithaca, New York, USA

Correspondence

Lawrence J. Bonassar, Department of Biomedical Engineering, 149 Weill Hall, Cornell University, Ithaca, NY 14853, USA.
Email: lb244@cornell.edu

Funding information

NIH, Grant/Award Numbers: 5R01AR071394-03, S10OD018516; NYSTEM, Grant/Award Number: CO29155; NSF, Grant/Award Numbers: CMMI-1536463, DMR-1807602; NIH-NIAMS, Grant/Award Numbers: 1R03AR075929-01, 5K08AR068470-02; NSF LEAP-HI, Grant/Award Number: CMMI 2245367; NSF CMMI, Grant/Award Number: 2225528/2225559; Harry M. Zweig Memorial Fund for Equine Research; Alfred P. Sloan Foundation; NSF MRSEC, Grant/Award Number: DMR-1719875

Abstract

Articular joints facilitate motion and transfer loads to underlying bone through a combination of cartilage tissue and synovial fluid, which together generate a low-friction contact surface. Traumatic injury delivered to cartilage and the surrounding joint capsule causes secretion of proinflammatory cytokines by chondrocytes and the synovium, triggering cartilage matrix breakdown and impairing the ability of synovial fluid to lubricate the joint. Once these inflammatory processes become chronic, posttraumatic osteoarthritis (PTOA) development begins. However, the exact mechanism by which negative alterations to synovial fluid leads to PTOA pathogenesis is not fully understood. We hypothesize that removing the lubricating macromolecules from synovial fluid alters the relationship between mechanical loads and subsequent chondrocyte behavior in injured cartilage. To test this hypothesis, we utilized an ex vivo model of PTOA that involves subjecting cartilage explants to a single rapid impact followed by continuous articulation within a lubricating bath of either healthy synovial fluid, phosphate-buffered saline (PBS), synovial fluid treated with hyaluronidase, or synovial fluid treated with trypsin. These treatments degrade the main macromolecules attributed with providing synovial fluid with its lubricating properties; hyaluronic acid and lubricin. Explants were then bisected and fluorescently stained to assess global and depth-dependent cell death, caspase activity, and mitochondrial depolarization. Explants were tested via confocal elastography to determine the local shear strain profile generated in each lubricant. These results show that degrading hyaluronic acid or lubricin in synovial fluid significantly increases middle zone chondrocyte damage and shear strain loading magnitudes, while also altering chondrocyte sensitivity to loading.

KEYWORDS

cartilage, lubrication, mechanobiology, mechanotransduction, tribology

Steven Ayala and Salman O. Matan contributed equally to this study.

1 | INTRODUCTION

Healthy synovial joints facilitate movement by providing a wear-resistant and low-friction surface through the combination of articular cartilage and synovial fluid.[1] The lubricity of synovial fluid is attributed to its macromolecule components specifically: lubricin, a mucinous glycoprotein; and hyaluronic acid (HA), a high-molecular-weight glycosaminoglycan.[2,3] The functional role of lubricin is to adhere to the cartilage surface, forming a network that generates an antiadhesive barrier capable of modulating contact between opposing cartilage surfaces.[4] HA acts as a high-viscosity lubricant that provides shock-absorbing, viscoelastic, and chondroprotective properties to synovial fluid; however, the specific lubricative mechanisms of HA are still largely unknown.[5–7] Together, lubricin and HA act to reduce shear stresses between cartilage surfaces, prevent chondrocyte death, and inhibit surface erosion.[2,8,9]

Joint health may become compromised following severe injury delivered to cartilage tissue and lead to posttraumatic osteoarthritis (PTOA) through increases of inflammation and downstream catabolic changes to the synovial fluid, extracellular matrix, and subchondral bone.[10,11] Following significant trauma, joint inflammation triggers the release of cytokines and enzymes including tumor necrosis factor α (TNFα), interleukin-1β (IL-1β), matrix metalloproteinases, reactive oxygen species, aggrecanase, and hyaluronidase.[10,12–14] These biological mediators result in mitochondrial (MT) depolarization, chondrocyte apoptosis, cell death, destruction of cartilage matrix, and changes in synovial fluid quality via loss of lubricin and degradation of HA.[7,15–18] Decreased concentrations of HA and lubricin reduce synovial fluid lubricity, leading to increases in friction, shear strains, and chondrocyte damage during articulation.[19,20] Furthermore, changes in synovial fluid are particularly interesting in the context of traumatic injury, as synovial inflammation has been shown to have a greater part in the pathophysiology of PTOA compared with idiopathic OA.[21] This phenomenon indicates the need to study the role of compromised synovial fluid in the development of PTOA.

Prior studies of cartilaginous injuries note levels of cellular and tissue damage are highest at the site of trauma, typically the cartilage surface, then subsiding in the surrounding area.[22] These incidences can create a dangerous feedback loop starting with degradation of synovial fluid, via increased secretion of inflammatory cytokines and enzymes, leading to increased joint friction, resulting in increased shear strain during joint articulation, triggering increased chondrocyte damage, thereby generating a greater inflammatory response.[8,23,24] Additionally, previous studies from our group have shown, via our ex vivo model of PTOA, that damage to the cartilage middle zone increases postinjury by subsequent articulation, due to the inability of the compromised surface region to protect the tissue bulk from increased shear strains.[25,26] Yet it is unknown how the effect of degraded synovial fluid further confounds the initial traumatic injury.

In the present study, we hypothesize that treating synovial fluid (SF) with trypsin and hyaluronidase will: (1) increase local strain in cartilage during sliding, (2) increase chondrocyte damage during sliding, and (3) negatively modulate the relationship between shear strain and subsequent chondrocyte damage in traumatically injured cartilage. Specifically, our objectives were to assess the effects of degrading HA and lubricin in synovial fluid on (1) the response of chondrocytes to sliding motion after impact injury; (2) shear strain profiles in cartilage during sliding motion; (3) the relationship between local shear strain and chondrocytes viability, apoptosis and MT polarization.

2 | MATERIALS AND METHODS

2.1 | Cartilage preparation

Cartilage from the femoral condyle of the knee joint of 12 neonatal (i.e., skeletally immature) bovids (sex unknown; Gold Medal Packing) was sterilely harvested, rinsed with Dulbecco's phosphate-buffered saline (PBS) containing antibiotics (100 U/mL penicillin-streptomycin, Mediatech) and sectioned into cylindrical plugs using 6 mm diameter biopsy punches (Integra). Explants from the femoral condyle were trimmed, while keeping the articular surface intact, to 2 mm in depth. Cuts were performed using a custom jig and blades lubricated with bovine synovial fluid (Lampire) to limit chondrocyte death preceding testing.[25] Before injury, explants tested via confocal microscopy were incubated overnight in media (phenol red-free dulbecco's modified eagle medium containing 1% fetal bovine serum [FBS], 4-(2-hydroxyethyl)-1-piperazineethanesulfonic acid 0.025 mL/mL, penicillin 100 U/mL, streptomycin 100 U/mL, and 2.5 mM glucose) at 37°C, 5% CO_2.

2.2 | Lubricant preparations

To observe the effect of poorly lubricating synovial fluid on subsequent cartilage shear strain and chondrocyte damage during articulation, synovial fluid was enzymatically degraded with either hyaluronidase (HAase) or trypsin (Try). Hyaluronidase treatment was used to catabolize HA, one of the main macromolecules attributed to synovial fluid lubrication, thereby decreasing synovial fluid viscosity.[3] Whereas, trypsin was used to deplete synovial fluid of its lubricin content, the second main macromolecule attributed to synovial fluid lubrication, thereby increasing the boundary friction coefficient between cartilage and articulating surface.[27,28] Bovine synovial fluid (SF) (Lampire) was incubated for 2 h at 37°C under constant stirring conditions with bovine testes hyaluronidase (25 µg/mL, 400–1000 U/mg, Sigma Aldrich) or trypsin EDTA (100 µL of 2 mg/mL, 0.25% trypsin, 0.1% EDTA, 1X, Mediatech) as previously reported.[29,30] To prevent enzymatic degradation from causing cartilage tissue degradation, both degraded lubricants were treated with a PI cocktail (Thermo Fisher Scientific) and used for confocal elastography testing on cartilage explants.

2.3 | Combined loading model of PTOA

Cartilage explants were subjected to injury using a previously described spring-loaded impactor system.[25,31] A single cycle of unconfined compression was delivered to the articular surface of explants using a 12 mm diameter cylindrical impacting tip. All impacts were delivered, over a loading time of ~1 ms, at a peak stress of 17.34 ± 0.99 MPa and peak stress rate of 21.6 ± 2.45 GPa/s. Loading magnitudes of this nature have been seen in previous studies to cause the failure of the anterior cruciate ligament, however, this loading protocol was chosen to deliver injurious compression resulting in pathological chondrocyte death and damage without full-thickness cracking.[32,33] Following traumatic injury, impacted cartilage explants were immediately slid against a polished glass counterface (McMaster Carr) in a custom-built tribometer.[28,34–36] Explants were submerged in a lubricating bath of either bovine SF, PBS, SF with hyaluronidase (SF+HAase), or SF with trypsin (SF+Try), compressed to 15% axial strain, allowed to equilibrate for 60 min, then slid for 60 min at 1 mm/s.[28] This loading regimen is known to be reliable at producing cell death, apoptosis, and MT depolarization.[25,28,31,35] The results of these groups were then compared with a control group that received no form of injury or manipulation.

2.4 | Confocal elastography

A setup mimicking the tribometer configuration was mounted on a 3i Marianas Spinning Disk Confocal Microscope (Carl Zeiss AG) to measure depth-dependent shear modulus and shear strains of cartilage explants.[37] Shear strains were tracked in a similar manner to previous studies that measured depth-dependent shear properties.[38] Cylindrical explants were axially bisected into hemicylinders that were stained for 1 h in 14 µg/mL 5-dichlorotriazinyl-aminofluorescein (5-DTAF, Molecular Probes) followed by a 30 min PBS wash. Samples were then mounted via their deep zone to a tissue deformation imaging stage (TDIS, Harrick Scientific) as previously described.[39,40] Samples were submerged in a lubricating bath of either bovine SF, PBS, SF+HAase, SF+Try, SF with hyaluronidase and protease inhibitors (SF+HAase& PI), or SF with trypsin and protease inhibitors (SF+Try& PI), compressed to 15% axial strain against polished glass using a micrometer stage, and allowed to stress relax for 30 min. In a similar manner to shearing performed on the tribometer, the glass slide was reciprocated against the cartilage surface using a piezoelectric positioning stage at a sinusoidal magnitude of 5% of sample thickness at 1 Hz. Videos were captured at 20 frames per second throughout the tissue depth to track the depth-dependent properties of the cartilage tissue. Depth-dependent shear deformations were tracked by analyzing the displacement of the tissue between frames via a custom MATLAB code. The maximum local shear strains were calculated through differentiation of the local displacements as previously described.[41,42]

2.5 | Confocal microscopy

Imaging of explants began 3 h postinjury. As described previously, cylindrical samples were axially bisected into hemicylinders and stained either for 30 min with 1 µL/mL Calcein AM and 1 µL/mL ethidium homodimer (Thermo Fisher Scientific), 30 min with CellEvent Caspase-3/7 Green (Thermo Fisher Scientific) following manufacturer instructions, or MitoTracker Green (200 nM; Thermo Fisher Scientific) for 20 min followed by addition of tetramethylrhodamine methyl ester perchlorate (10 nM; Thermo Fisher Scientific) for 30 min.[24,25] After staining, all explants were rinsed in PBS for 30 min. Cartilage explants were imaged on a Zeiss LSM880 confocal/multiphoton inverted microscope to determine the cellular response of femoral condylar cartilage to rapid impact injury followed by repeated frictional shear while submerged in compromised synovial fluid.

Confocal images were captured and imported into ImageJ to create a composite image (550 µm wide vs. 725 µm depth). Depth-dependent cellular responses were quantified using Fiji (NIH) a custom MATLAB program (MathWorks, Inc.).[43,44] Global tissue responses were reported as percent cell death, percent cells with depolarized MT, and number of caspase-positive cells normalized to the area of composite image: 0.399 mm^2. Depth-dependent results were calculated by segmenting each image into 18 ~40 µm bins to include enough cells to represent the response at the tissue surface. The number of caspase-positive cells were normalized to the area of the bin, 0.022 mm^2.

2.6 | Statistical analysis

One-way analysis of variance (ANOVAs) were performed to compare the global effect of poor lubricating synovial fluid on the spatial patterns of cellular response in femoral condylar cartilage while repeated measures two-way ANOVAs were used to compare depth-dependent results. Differences were considered statistically significant at $p \leq 0.05$, for both global tissue and depth-dependent results. Pairwise comparisons between groups were performed using Tukey's honestly significant difference (HSD) method. Depth-dependent results were fit to a previously described stretched exponential model where the results of each stain were plotted as a function of distance away from the cartilage articular surface.[25] Goodness of fit between the data and the model was characterized by R^2 values. Two-way ANOVAs and Tukey's HSD tests were then used to compare the values of the coefficients of this nonlinear model between all groups. Significant differences between shear strain maps for each group were determined using repeated measures two-way ANOVA and Tukey's HSD tests, while differences between degraded synovial fluid shear strains and their counterparts treated with protease inhibitors (PIs) were determined using a standard two-way ANOVA and Tukey's HSD tests.

Depth-dependent shear strains were plotted against depth-dependent results for each cell damage metric, with coefficient of determination, represented by R^2 values, being calculated by modeling the data to a line of best fit. Differences of slopes between SF, SF+HAase, and SF+Try groups were tested using an interaction model, p values associated with the interactions were Bonferroni adjusted and differences were considered statistically significant at $p \leq 0.05$. Nonlinear modeling, correlation plots, and statistical analyses were performed using GraphPad Prism 10 (Figure 1).

3 | RESULTS

3.1 | Confocal microscopy

Unloaded control cartilage showed high viability, minimal apoptosis, and polarized mitochondria throughout tissue depth. All impacted and slid samples showed some amount of cell death, apoptosis, and mitochondrial depolarization, primarily at the tissue surface. Samples slid in PBS showed the highest levels of cell damage, penetrating into the middle zone, those slid in SF had minimal cell death and apoptosis, with some MT depolarization with 200 µm of the surface. Samples articulated with SF degraded by hyaluronidase or trypsin were most similar to those slid in PBS, with slightly less cell damage (Figure 2).

Global magnitudes of cell death, apoptosis, and MT depolarization for the control group (8.12%, 180 apoptotic cells/mm^2, 12.47%) were shown to be low, allowing for a reasonable assumption that additional damage displayed by treated groups is the result of the combined injury model (Figure 3). Bulk tissue analysis of cellular damage metrics showed significant increases in cell death ($p < 0.01$), apoptosis (other than SF ($p < 0.005$)), and MT depolarization ($p < 0.0002$) for SF, SF+HAase, SF+Try, and PBS when compared with control cartilage samples (Figure 3A, C, E). However, significant increases in chondrocyte damage between degraded synovial fluid groups and normal SF only existed between SF+HAase and SF in apoptosis measurements ($p = 0.0036$), 907 versus 488 apoptotic cells/mm^2, respectively (Figure 3C). All other bulk tissue comparisons between degraded synovial fluid groups and normal SF yielded nonsignificant results ($p > 0.05$). All global metrics were not different between PBS and SF degraded with either hyaluronidase or trypsin.

Depth-dependent analysis showed that depleting the lubricating properties of synovial fluid caused significantly more damage to chondrocytes across the region of interest compared with what is expected from traumatic injury alone (Figure 3B, D, F). Sliding traumatically injured cartilage samples in non-degraded SF resulted in significantly greater cell death, apoptosis, and MT depolarization compared with uninjured controls at the cartilage surface up to ~300 µm, while in the middle zone only MT depolarization significantly increased specifically from ~500 to 700 µm ($p < 0.05$). However, both SF+HAase and SF+Try caused additional regions of cartilage tissue to experience greater chondrocyte damage compared with uninjured controls. SF+HAase resulted in greater cell death up to 340 µm (minimum of 35%) except in between 220 and 300 µm and showed significance from 500 to 700 µm ($p < 0.0140$). While SF+Try showed higher cell death up to 140 µm (minimum of 42%) and SF (minimum of 38%) resulting in greater cell death up to only 261 µm ($p < 0.0343$) (Figure 3B). We observed a significant difference in cell death between SF and PBS throughout the tissue ($p < 0.05$).

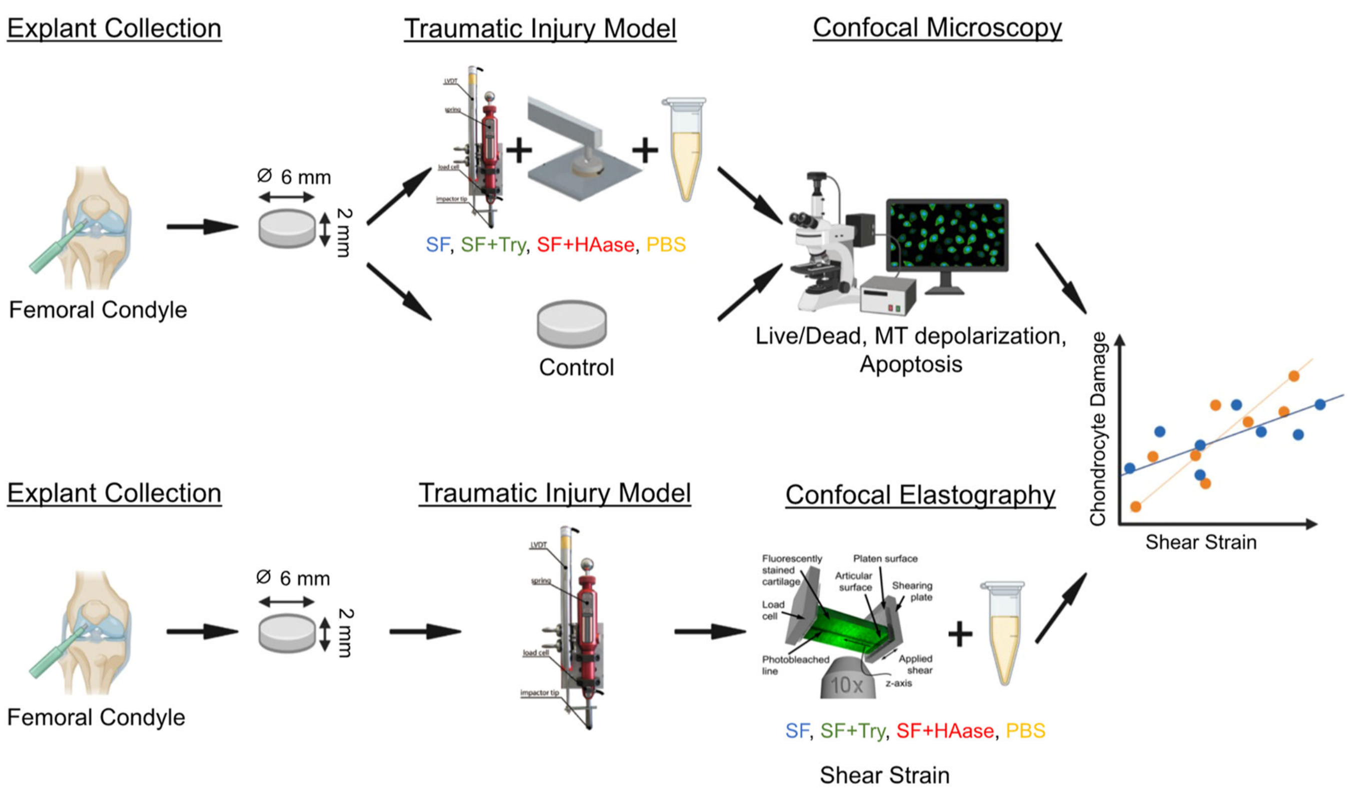

FIGURE 1 Experimental design and methods.

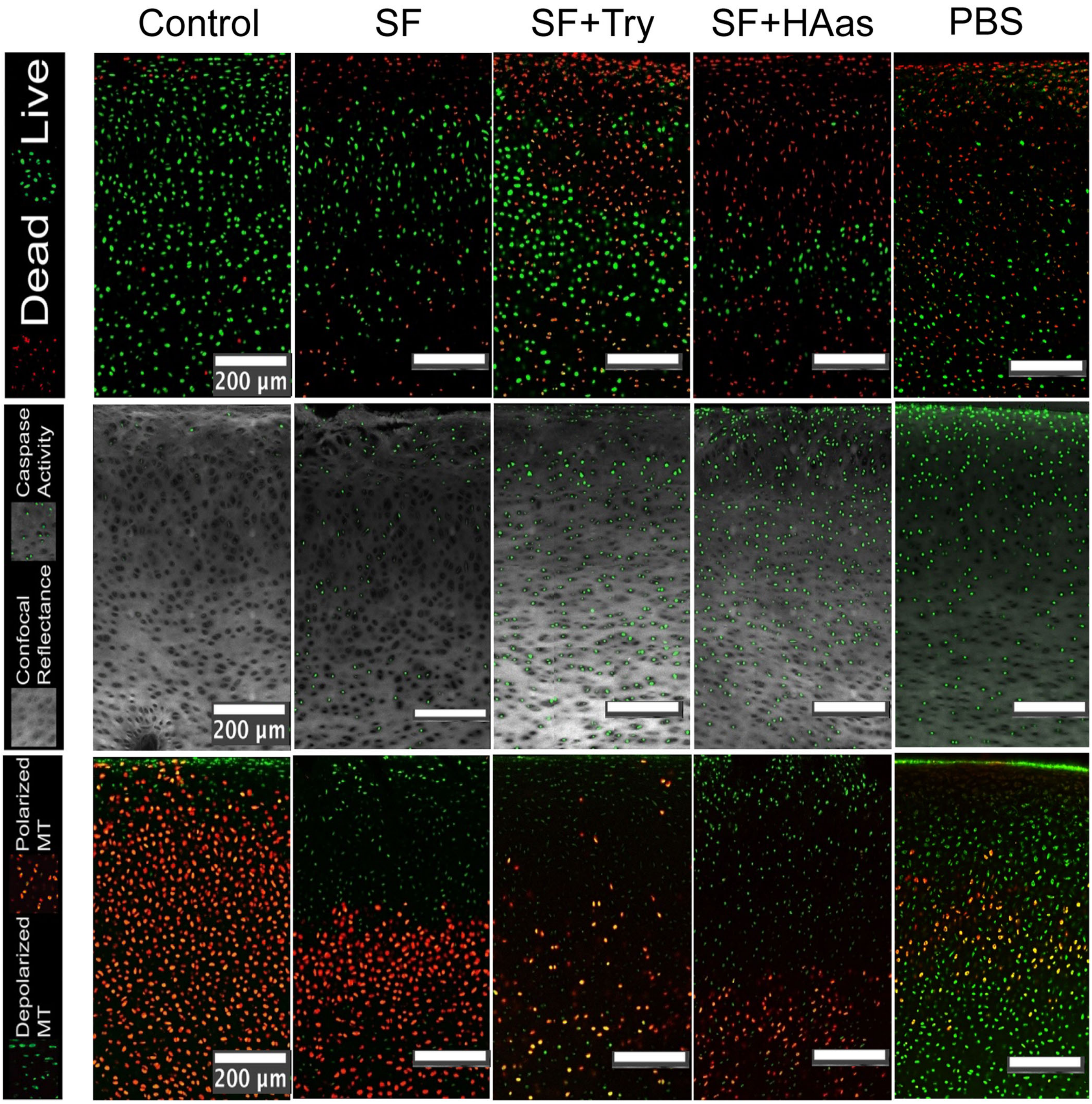

FIGURE 2 Representative confocal images of all groups. Top row: green represents the live cells while red represents dead cells. Middle row: the gray is confocal reflectance while green is cells showing caspase activity. Bottom row: orange/red is polarized mitochondrial (MT), and green is depolarized MT.

Meanwhile, there were no significant differences in cell death, at any region of the cartilage, between samples slid in degraded SF and those slid in standard SF or between SF+HAase and SF+Try ($p > 0.05$). Caspase activity measurements revealed that SF+HAase and SF+Try resulted in significantly greater chondrocyte apoptosis, compared with uninjured controls, from the cartilage surface up to 400 µm ($p < 0.0286$) (Figure 3D). Levels of apoptosis in this region ranged from 2398 to 784 apoptotic cells/mm^2 for the SF+HAase group, and 1912 to 694 apoptotic cells/mm^2 for the SF+Try group. Conversely, injured cartilage samples slid in PBS produced caspase activity greater than controls up to 80 µm ($p < 0.0197$), the level of apoptosis in this region is ranged between 3851 and 1248 apoptotic cells/mm^2. However, the SF slid samples showed chondrocyte apoptosis at a similar level to control samples ($p > 0.05$) across all the depths. Additionally, SF+HAase and SF+Try groups generated greater levels of chondrocyte apoptosis compared with SF from the articular

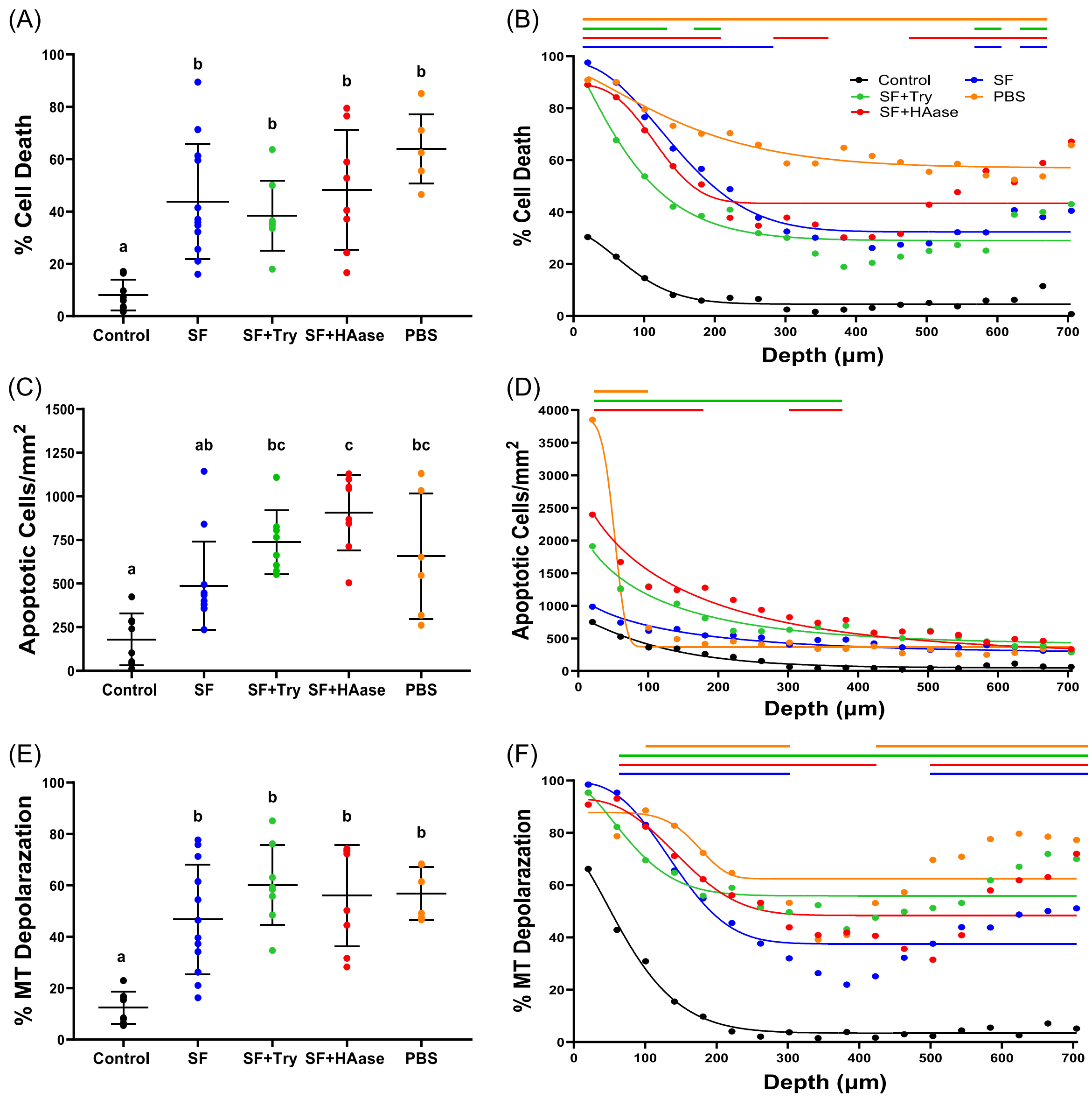

FIGURE 3 Bulk tissue and depth-dependent cellular response results with nonlinear model curve fit. (A) Percent cell depth for all the groups. (B) Depth-dependent cell death for all the groups. (C) Number of apoptotic cells per mm^2 for all the groups. (D) Depth-dependent apoptotic cells for all the groups. (E) Percent mitochondrial (MT) depolarized for all groups. (F) Depth-dependent MT depolarization for all the groups. Groups with different letters denote a significant difference between them ($p < 0.05$), while the colored lines above each graph show regions of tissue where a group shows a significant difference between itself and the control group. $n = 6–12$.

surface up to 200 and 100 μm ($p < 0.0243$), respectively. Lastly, the magnitude of MT depolarization in all the groups showed no significance in the first 40 μm of the tissue. The MT depolarization of the SF group was significantly greater than controls from 40 to 260 μm and 500 to 700 μm ($p < 0.0417$) (Figure 3F). Surface zone depolarization ranged from 99% to 71% and the middle zone depolarization ranged from 3% to 62%, showing an increasing trend within the middle zone. However, SF+HAase showed significantly enhanced MT depolarization from 40 to 440 μm (93%–41%) and 520 to 700 μm (41%–72%) ($p < 0.0477$) while SF+Try showed enhanced depolarization across the entire region of interest (minimum of 43%) ($p < 0.0257$), both compared with the control group. In contrast, the PBS-treated group showed an increase in depolarization from 80 to 280 μm (89%–52%) and from 400 to 700 μm (53%–77%) compared with the control group ($p < 0.0417$). SF+Try treated group showed a significant difference compared with the control group through the tissue depth other than the first 40 μm of the surface tissue. Similarly, SF+HAase and SF+Try groups both showed an increasing trend of MT depolarization within the cartilage middle zone. No significant intergroup differences in MT depolarization were observed between SF, SF+HAase, and SF+Try ($p > 0.05$).

Depth-dependent microscopy data were fit to the nonlinear function, $y(x) = P + (Y_o - P) \times e^{-(x/\lambda)^d}$, to quantify average levels of chondrocyte damage as a function of depth. Group comparisons of the parameters of our nonlinear model can be observed in Figure 3 and numerical results can be seen in Table 1. The comparison between groups on the results of Table 1 is reported in Figure 4. The magnitude of damage at the articular surface, represented by Y_o, showed no significant differences between any groups in the case of apoptosis and MT depolarization ($p > 0.05$). However, the magnitude of cell death at the articular surface for SF, SF+HAase, SF+Try, and PBS were all significantly greater than that of the control group ($p < 0.0024$). The amount of cell death seen at the surface zone between these groups ranged from 89% to 99%, while the control group was at 32%. There were no significant differences between noncontrol groups in Y_o for any of the three metrics of chondrocyte damage ($p > 0.05$). The magnitude of damage at the middle zone, P, showed multiple significant differences between groups in cell death and MT depolarization measurements. For cell death, not only were SF, SF+HAase, SF+Try, and PBS all significantly greater than the control group ($p < 0.0001$), but both SF+HAase and PBS were greater than SF ($p = 0.0033$) and ($p < 0.0001$), respectively (Figure 4B). SF+HAase also possessed a significantly higher p value than SF+Try ($p = 0.0004$) and PBS ($p = 0.0019$). For MT depolarization, while we once again see SF, SF +HAase, SF+Try, and PBS were significantly greater than the control group ($p < 0.0001$). In this case, PBS, SF+HAase, and SF+Try possessed significantly greater middle zone damage compared with SF (Figure 4H). SF+HAase were not significantly different compared with SF+Try ($p = 0.37$), but significantly different compared with PBS ($p = 0.023$). We note no significant differences between any groups in p for apoptosis measurements ($p > 0.05$). Finally, the characteristic length scale, λ, for the transition between Y_0 and P, showed no significant differences between groups ($p > 0.05$).

3.2 | Confocal elastography

Using less viscous and less lubricious synovial fluid produced significantly greater shear strains, particularly at the cartilage surface (Figure 5). Injured cartilage samples that were slid in PBS, SF+HAase, and SF+Try resulted in shear strains at the cartilage surface that were 66.6%– 224% greater than the SF group ($p < 0.0068$). This trend continued for PBS, SF+HAase, and SF+Try up to a depth of 85 µm ($p < 0.05$). After which local strains were not different between groups. To demonstrate that protease treatment did not damage cartilage during sliding we compared these groups to those in which PIs were added before sliding. No difference in local strains was observed with

TABLE 1 Results of nonlinear model curve fit of confocal microscopy data.

$y(x) = P + (Y_o - P) \times e^{-(x/\lambda)^d} + P$

Stain/Group	N	Y_o	SEM	P	SEM	λ	SEM	d	SEM	R^2
Live/Dead										
Control	8	1	4.24	4.54	0.76	98.52	15.27	1.73	0.66	0.9048
SF	12	97.26	4.80	32.34	1.58	173.33	12.90	2.01	0.42	0.9625
SF+Try	8	97.76	18.27	29.01	2.51	98.75	30.95	1.22	0.60	0.8587
SF+HAase	8	88.99	10.81	43.35	3.17	133.39	27.82	2.79	2.28	0.6837
PBS	6	94.25	5.60	57.02	2.10	184.80	32.38	1.31	0.46	0.9075
Apoptosis										
Control	8	830.97	88.53	49.12	17.53	126.18	17.40	1.10	0.23	0.9696
SF	12	1189.72	250.71	273.82	84.74	139.94	46.11	0.76	0.37	0.9087
SF+Try	8	2307.37	514.01	400.31	110.27	112.64	40.23	0.76	0.32	0.9435
SF+HAase	8	2969.14	616.48	239.11	237.78	149.07	39.59	0.76	0.32	0.9333
PBS	6	3852.00	80715.4	371.47	28.44	55.99	1949.5	4.34	1773.8	0.9858
MT depolarization										
Control	8	71.40	3.88	3.41	0.62	99.12	6.07	1.49	0.19	0.9888
SF	12	99.17	8.31	37.56	2.73	160.11	19.71	2.59	1.51	0.8690
SF+Try	8	98.25	14.57	55.90	2.45	95.87	33.75	1.67	1.38	0.6719
SF+HAase	8	92.91	9.95	48.44	3.45	170.55	34.91	2.60	1.93	0.7018
PBS	6	87.75	8.63	62.48	3.91	184.19	44.42	5.73	10.79	0.4046

Note: Live/Dead and MT Depolarization are reported as percentages while apoptosis is reported as # of cells/mm^2.
Abbreviations: MT, mitochondrial; PBS, phosphate-buffered saline; SF, synovial fluid.

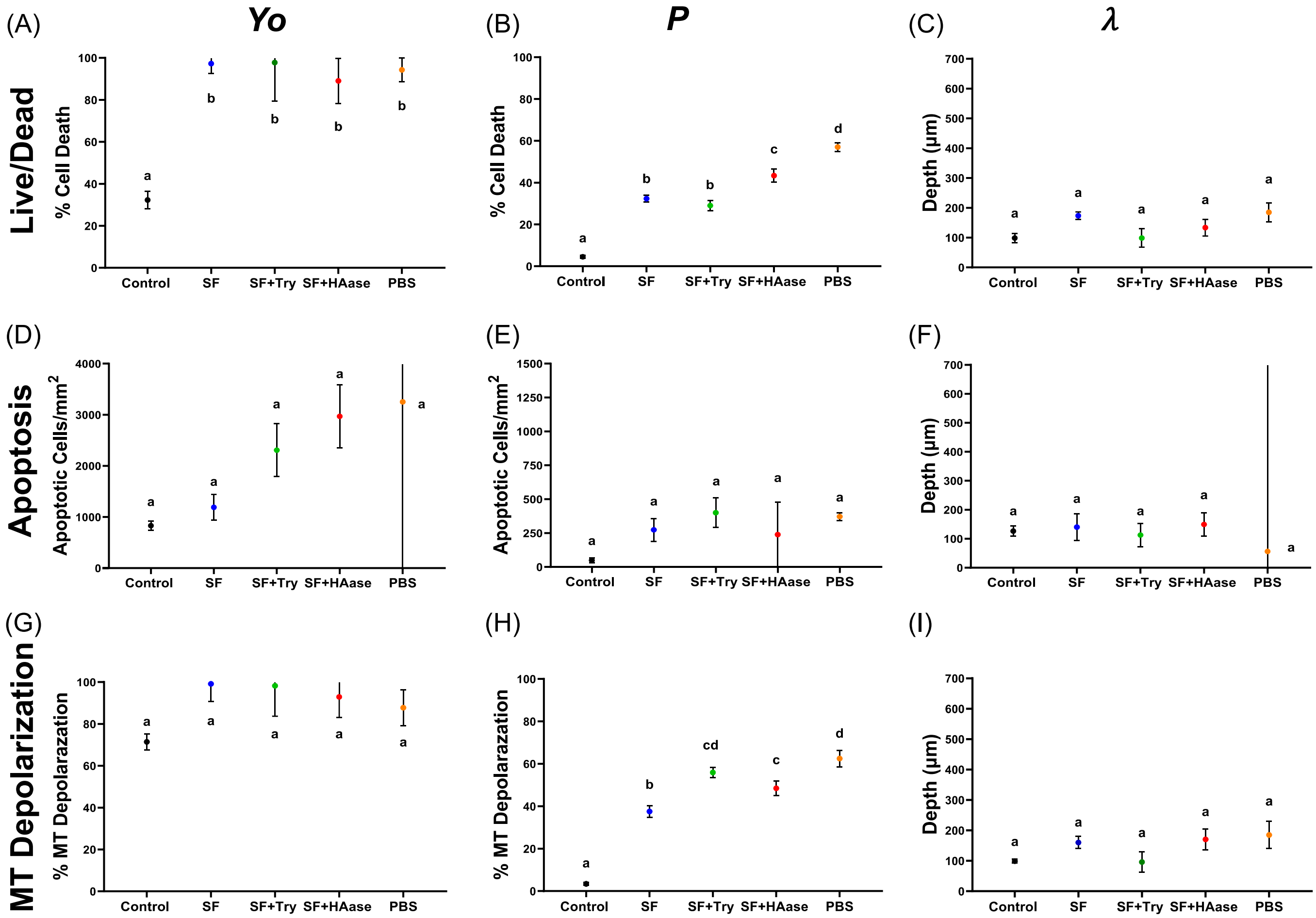

FIGURE 4 Comparison of parameters from nonlinear model of the spatial patterns of chondrocyte damage, indicating damage at the articular surface (Y_0) and deeper into the tissue (P) as well as the characteristic length scale of the transition between these values (λ) for respectively cell death (A, B, C), apoptosis (D, E, F), and mitochondrial depolarization (G, H, I) Groups with different letters denote significant difference ($p < 0.05$), $n = 6$–12.

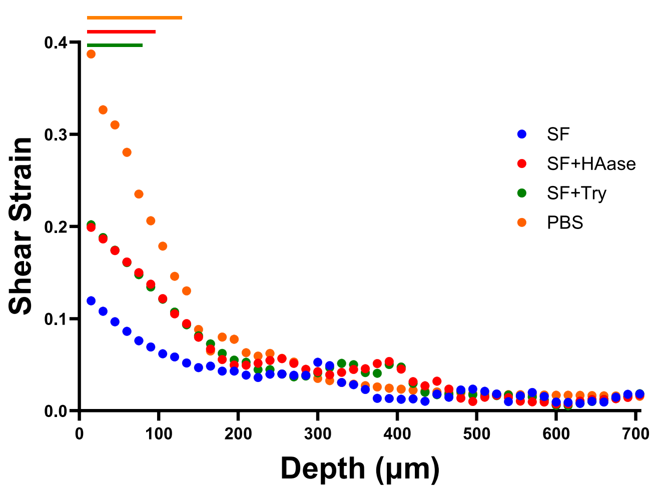

FIGURE 5 Depth-dependent shear strains for lubricant groups used in the study, lines above indicate areas of significant difference between the SF group and the group indicated by line color ($p < 0.05$). $n = 6$–8. SF, synovial fluid.

or without PI ($p > 0.05$), indicating that the cartilage was not degraded by these enzymes (Supporting Information S1: Figure 1).

3.3 | Chondrocyte damage vs shear strain

After performing confocal elastography and microscopy analysis, local cell death, apoptosis, MT depolarization, and shear strain were registered to the same local region of 40 µm depth. Each cellular injury metric was plotted against shear strain data to generate plots that show the magnitude of damage for a given level of mechanical load, thereby displaying the sensitivity of chondrocytes to shear strain. Chondrocytes sensitivity to shear strain was represented as the slope of the linear trendline for each group. Correlation plots revealed shear strain was a strong predictor of chondrocyte fate, regardless of which lubricant was used. Detail on the results of linear regression analysis, for all data sets, can be seen in Table 2. The relationship between chondrocyte damage and shear strain displayed strong R^2 values ranging between 0.3649 and 0.7395 and the p value

TABLE 2 Results from fitting shear strain vs chondrocyte fate data to linear regression model.

	$y(x) = mx + b$									
	Stain/Group	N_x	N_y	m	SEM	b	SEM	R^2	Slope comparison	b value comparison
Live/Dead	Pooled data	8	8/12	209.50	28.96	38.64	2.41	0.4277	-	
	SF	8	12	712.20	82.11	20.69	3.69	0.8246	a	a
	SF+Try	8	8	286.70	43.39	22.20	3.26	0.7318	b	a
	SF+HAase	8	8	231.20	62.25	38.14	4.69	0.4629	b	b
	PBS	6	6	111.0	11.15	57.53	1.34	0.8608	b	c
Apoptosis	Pooled data	8	8/12	7524.00	533.7	274.40	44.41	0.7395	-	-
	SF	8	12	5745.00	604.80	282.80	27.20	0.8494	a	a
	SF+Try	8	8	7375.00	449.00	336.70	33.69	0.9440	ab	ab
	SF+HAase	8	8	9338.00	748.50	394.10	56.39	0.9068	bc	ab
	PBS	6	6	7533.00	1073.00	55.25	128.60	0.7549	ab	ac
MT depolarization	Pooled data	8	8/12	180.80	28.52	49.28	2.37	0.3649	-	-
	SF	8	12	663.90	114.40	25.97	5.15	0.6778	a	a
	SF+Try	8	8	173.70	45.46	51.48	3.41	0.4771	b	b
	SF+HAase	8	8	263.60	57.89	43.27	4.36	0.4643	b	bc
	PBS	6	6	91.85	34.29	61.61	4.11	0.3096	b	bd

Note: Live/Dead and MT Depolarization are reported as percentages while Apoptosis is reported as the number of cells/mm^2. SEM represents the standard error of the mean and R^2 represents the correlation between the linear regression and experimental values. Rows that shared colors have slopes and b values compared via one-way ANOVA. Different letters indicate $p < 0.05$.

Abbreviations: ANOVA, analysis of variance; MT, mitochondrial; PBS, phosphate-buffered saline; SF, synovial fluid.

is from $p < 0.00001$ to $p < 0.00001$ for pooled data (Figure 5A, C, E). For cell death, apoptosis, and MT depolarization measurements the sensitivities of chondrocytes to shear strain for all datasets pooled together were 209.5%, 7524 apoptotic cells/mm^2, and 180.8%, respectively. Separating the data by lubricant group revealed that removing the lubricating macromolecules of synovial fluid alters the sensitivity of chondrocytes to shear strain (Figure 5B,D,F). The sensitivities of the SF group for cell death, apoptosis, and MT depolarization plots were 712.20%, 5745 apoptotic cells/mm^2, and 663.90%, respectively. The SF group showed significantly lower apoptosis sensitivity compared with SF+HAase ($p < 0.0001$) and SF +Try ($p = 0.0302$). The SF group also showed significantly higher cell death ($p = 0.0003$) and MT depolarization ($p = 0.0006$) sensitivity compared with the SF+Try group, and no significant difference in apoptosis sensitivity ($p = 0.1791$) compared with the SF+Try group. R^2 values for all three lubricants for each chondrocyte fate metric ranged between 0.3096 and 0.9440 with a p value from $p < 0.0164$ to $p < 0$ 00001, again showing a high degree of correlation between shear strain and cell damage.

4 | DISCUSSION

In this body of work, we have shown that inhibiting distinct synovial lubricating mechanisms, specifically degrading synovial fluid HA and lubricin, resulted in increased shear strains during cartilage articulation, leading to enhanced chondrocyte damage. We note that modulating the quality of synovial fluid resulted in significant changes in the spatial patterns of chondrocyte damage compared with healthy tissue, and even compared with traumatically injured cartilage. This result was seen regardless of whether HA or lubricin was removed from synovial fluid, indicating that both macromolecules are essential to ensure maximal protection of cartilage tissue. Both enzymatic treatments resulted in greater cell death, apoptosis, and MT depolarization compared with normal synovial fluid, particularly at the middle zone. Furthermore, enzymatic treatment of the lubricating macromolecules in synovial fluid resulted in significant changes in chondrocyte sensitivity to shear strain. Ultimately, these results suggest that the role of synovial inflammation in the context of PTOA is to propagate cellular injury into deeper regions of cartilage tissue, which would normally be shielded by healthy synovial fluid.

Decreasing the lubricating quality of synovial fluid resulted in greater chondrocyte damage throughout the middle zone of cartilage tissue, but minimal change to the damage at the surface region. Studies have shown that in uninjured cartilage tissue, poor quality lubricants generate higher friction and shear strains during

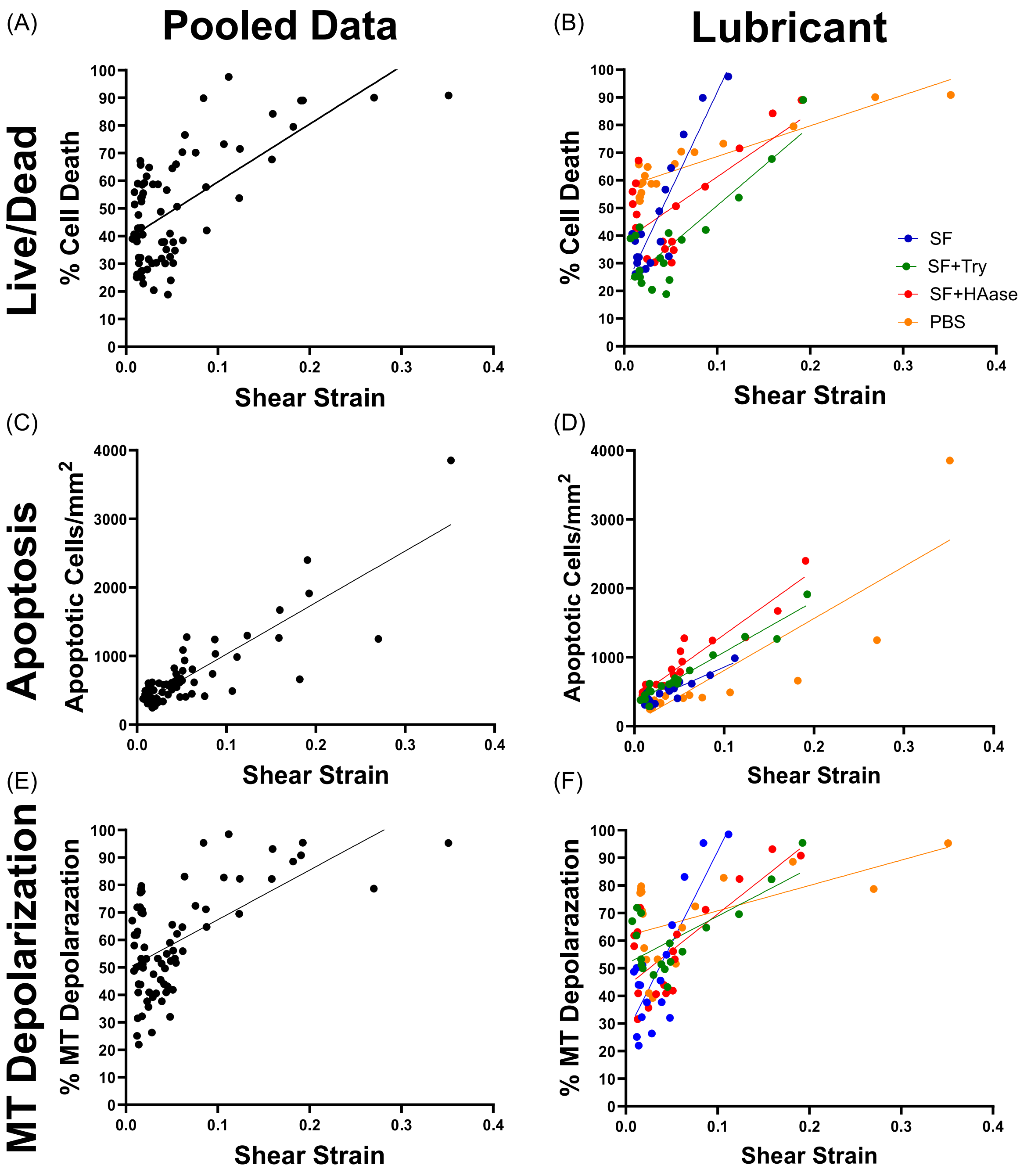

FIGURE 6 Correlation plots of local shear strain against magnitude of cellular responses. (A) Percent cell death of all data pooled together. (B) Percent cell death with lubricant used. (C) Number of apoptotic cells per mm^2 with all the data pooled together. (D) Number of apoptotic cells per mm^2 with lubricant used. (E) Percent mitochondrial (MT) depolarization with all the data pooled together. (F) Percent MT depolarization with lubricant used. Statistical analysis between lubricant groups is performed by comparing slopes of linear trendlines fit to each group. Significant differences appear as intersections between lines of different groups, whereas nonsignificant comparisons result in parallel lines. *y* axis *n* = 6–12, *x* axis *n* = 6–8.

articulation causing greater cellular damage near the articular surface.[7,23,24] The results showed an increase of shear strain at 150 µm of tissue surface of 66%–224% for SF treated with HAase and trypsin and PBS. However, our injury model has been shown to result in the death and damage of an overwhelming majority of chondrocytes up to a minimum of 200 µm from the surface.[25] Increased shear strains at the surface caused by poorly lubricating synovial fluid resulted in minimal additional surface zone chondrocyte damage because impact injury had already compromised this region. Instead, removing HA and lubricin from synovial fluid appeared to decrease fluid lubrication such that depth-dependent shear strain increased, leading to increased damage propagation into deeper regions of the cartilage tissue. In addition to the mechanical role of synovial fluid in maintaining joint health, it is important to note potential biological mechanisms by which degraded synovial fluid may facilitate the propagation of cellular damage in cartilage. For example, there is evidence to suggest that catabolism of high-molecular-weight HA into smaller oligomers triggers increased production of reactive oxygen species, proinflammatory cytokines, and hyaluronidase by macrophages, synoviocytes, and chondrocytes.[45–48] Focal defects generated during trauma may allow a pathway for low-molecular-weight HA that exists within the synovium to reach middle zone chondrocytes they could not normally. Furthermore, lubricin also possess chondroprotective qualities and its removal is associated with enhanced apoptosis, degradative enzyme production, and decreased lubricin secretion by chondrocytes.[49–51]

Degradation of HA and lubricin from synovial fluid caused significant changes in the sensitivity of chondrocytes to shear strain as manifested in cell death, apoptosis, and MT depolarization. Decreasing the lubricating properties of SF resulted in shear strains almost twice as high from baseline injury at the articular surface. This change resulted in an increased baseline in cell damage before the initiation of sliding, but lower sensitivity to sliding-induced shear strains as reflected by the slope of the curves for cell death and MT depolarization (Figure 6). These results are consistent with previous studies that suggest osteoarthritic changes cause chondrocytes to become more susceptible to inflammatory cytokines, reactive oxygen species, and mechanical stimuli.[52–54] These findings reinforce the theory of a positive feedback loop of PTOA progression where traumatic injury compromises cartilage tissue such that there is an increase of mechanical load and inflammatory cytokines that cause destruction of both chondrocytes and cartilage tissue, thereby triggering greater local strains and increased release of inflammatory cytokines until the disease progresses to its end-stage.[55–57]

While this study provides exciting new insight on the role of synovial fluid in the manifestation of PTOA, it is not without its limitations. These limitations include an inability to examine the long-term effects of degrading synovial fluid. The biological mechanisms by which synovial fluid interacts with chondrocytes and the surrounding matrix may not be fully captured over the timescale that cartilage explants were exposed to the lubricants used in this study.[58–60] Nevertheless, the mechanical effects of synovial fluid degradation (i.e., increasing local cartilage tissue strains, particularly at the surface) largely explained the changes in chondrocyte response between lubricant groups. Additionally, trypsin and HAase were used to degrade protein and HA in SF to compromise lubrication. We did not directly confirm protein and HA degradation, but it is clear that lubrication was compromised by an increase in local tissue strain. Lastly, the particular enzymatic degradation of lubricin and HA in these studies may not reflect the quality of synovial fluid in the subacute-acute timescale of PTOA pathogenesis.[12,61]

In conclusion, the results of this study suggest that while the dominant effect in the manifestation of PTOA pathogenesis is the initial trauma generated during injury, removal of lubricin and HA synovial inflammation raises the magnitudes of shear strains and chondrocyte damage generated during articulation. This insight suggests synovial inflammation may be particularly threatening within the context of PTOA progression, compared with that of idiopathic OA. Furthermore, these conclusions indicate that early clinical application of viscosupplement lubricants may be an important strategy for treating PTOA. Finally, we observed minimal differences between synovial fluid with catabolized lubricin or HA, indicating that these macromolecules act together to achieve optimal joint lubrication and functionality. Through this work, we have advanced our ex vivo model of PTOA by considering synovial inflammation and in future studies, this model may serve as a platform to test the efficacy of disease-modifying treatments.

AUTHOR CONTRIBUTIONS

Steven Ayala, Salman O. Matan, Michelle L. Delco, Lisa A. Fortier, Itai Cohen, and Lawrence J. Bonassar contributed to experimental design, data analysis, manuscript writing, and manuscript editing. Steven Ayala and Salman O. Matan performed all experiments.

ACKNOWLEDGMENTS

The authors thank NIH 5R01AR071394-03, NYSTEM CO29155, NIH S10OD018516, NSF CMMI-1536463, NSF DMR-1807602, NIH-NIAMS 1R03AR075929-01, NIH-NIAMS 5K08AR068470-02, NSF LEAP-HI CMMI 2245367, NSF CMMI 2225528/2225559, Harry M. Zweig Memorial Fund for Equine Research, Alfred P. Sloan Foundation. This work made use of the Cornell Center for Materials Research Shared Facilities which are supported through the NSF MRSEC program (DMR-1719875).

CONFLICT OF INTEREST STATEMENT

Dr. Bonassar is a cofounder of and holds equity in 3DBio Corp.

ORCID

Steven Ayala http://orcid.org/0000-0003-2372-5680
Michelle L. Delco http://orcid.org/0000-0003-0973-2075
Lawrence J. Bonassar http://orcid.org/0000-0003-1094-6433

REFERENCES

1. Desrochers J, Amrein MW, Matyas JR. Microscale surface friction of articular cartilage in early osteoarthritis. *J Mech Behav Biomed Mater*. 2013;25:11-22.
2. Jay GD. Characterization of a bovine synovial fluid lubricating factor. I. Chemical, Surface activity and lubricating properties. *Connect Tissue Res*. 2009;28(1-2):71-88. doi:10.3109/03008209209014228
3. Balazs EA, Watson D, Duff IF, Roseman S. Hyaluronic acid in synovial fluid. I. Molecular parameters of hyaluronic acid in normal and arthritis human fluids. *Arthritis Rheum*. 1967;10(4):357-376. doi:10.1002/art.1780100407
4. Jay GD, Torres JR, Rhee DK, et al. Association between friction and wear in diarthrodial joints lacking lubricin. *Arthritis Rheum*. 2007;56(11):3662-3669. https://pubmed.ncbi.nlm.nih.gov/17968947/
5. Gupta RC, Lall R, Srivastava A, Sinha A. Hyaluronic acid: molecular mechanisms and therapeutic trajectory. *Front Vet Sci*. 2019;6(JUN):192.
6. Tamer TM. Hyaluronan and synovial joint: function, distribution and healing. *Interdiscip Toxicol*. 2013;6(3):111-125.

7. Bonnevie ED, Galesso D, Secchieri C, Bonassar LJ. Degradation alters the lubrication of articular cartilage by high viscosity, hyaluronic acid-based lubricants. *J Orthop Res*. 2018;36(5):1456-1464.
8. Waller KA, Zhang LX, Elsaid KA, Fleming BC, Warman ML, Jay GD. Role of lubricin and boundary lubrication in the prevention of chondrocyte apoptosis. *Proc Natl Acad Sci*. 2013;110(15):5852-5857.
9. Jones ARC, Gleghorn JP, Hughes CE, et al. Binding and localization of recombinant lubricin to articular cartilage surfaces. *J Orthop Res*. 2007;25(3):283-292.
10. Martel-Pelletier J, Barr AJ, Cicuttini FM, et al. Osteoarthritis. *Nat Rev Dis Primers*. 2016;2:16072. www.nature.com/nrdp
11. Ulrich-Vinther M, Maloney MD, Schwarz EM, Rosier R, O'Keefe RJ. Articular cartilage biology. *J Am Acad Orthop Surg*. 2003;11(6):421-430.
12. Catterall JB, Stabler TV, Flannery CR, Kraus VB. Changes in serum and synovial fluid biomarkers after acute injury (NCT00332254). *Arthritis Res Ther*. 2010;12(6):R229. https://arthritis-research.biomedcentral.com/articles/10.1186/ar3216
13. de Lange-Brokaar BJE, Ioan-Facsinay A, van Osch GJVM, et al. Synovial inflammation, immune cells and their cytokines in osteoarthritis: a review. *Osteoarthritis Cartilage*. 2012;20(12):1484-1499.
14. Delco ML, Bonnevie ED, Bonassar LJ, Fortier LA. Mitochondrial dysfunction is an acute response of articular chondrocytes to mechanical injury. *J Orthop Res*. 2018;36:739-750.
15. Punzi L, Galozzi P, Luisetto R, et al. Post-traumatic arthritis: overview on pathogenic mechanisms and role of inflammation. *RMD Open*. 2016;2(2):e000279. https://pubmed.ncbi.nlm.nih.gov/27651925/
16. Bartell LR, Fortier LA, Bonassar LJ, et al. Mitoprotective therapy prevents rapid, strain-dependent mitochondrial dysfunction after articular cartilage injury. *J Orthop Res*. 2019;38(6):1-11. doi:10.1002/jor.24567
17. Stevens AL, Wishnok JS, White FM, Grodzinsky AJ, Tannenbaum SR. Mechanical injury and cytokines cause loss of cartilage integrity and upregulate proteins associated with catabolism, immunity, inflammation, and repair. *Mol Cell Proteomics*. 2009;8(7):1475-1489.
18. Elsaid KA, Fleming BC, Oksendahl HL, et al. Decreased lubricin concentrations and markers of joint inflammation in the synovial fluid of patients with anterior cruciate ligament injury. *Arthritis Rheum*. 2008;58(6):1707-1715.
19. Kosinska MK, Ludwig TE, Liebisch G, et al. Articular joint lubricants during osteoarthritis and rheumatoid arthritis display altered levels and molecular species. *PLoS One*. 2015;10(5):e0125192. https://pubmed.ncbi.nlm.nih.gov/25933137/
20. Temple-Wong MM, Ren S, Quach P, et al. Hyaluronan concentration and size distribution in human knee synovial fluid: variations with age and cartilage degeneration. *Arthritis Res Ther*. 2016;18(1):18.
21. Thomas NP, Wu WJ, Fleming BC, Wei F, Chen Q, Wei L. Synovial inflammation plays a greater role in post-traumatic osteoarthritis compared to idiopathic osteoarthritis in the hartley Guinea pig knee. *BMC Musculoskelet Disord*. 2017;18(1):556. https://pubmed.ncbi.nlm.nih.gov/29284451/
22. Tochigi Y, Buckwalter JA, Martin JA, et al. Distribution and progression of chondrocyte damage in a whole-organ model of human ankle intra-articular fracture. *J Bone Joint Surg Am*. 2011;93(6):533-539.
23. Irwin RM, Feeney E, Secchieri C, et al. Distinct tribological endotypes of pathological human synovial fluid reveal characteristic biomarkers and variation in efficacy of viscosupplementation at reducing local strains in articular cartilage. *Osteoarthritis Cartilage*. 2020;28(4):492-501. doi:10.1016/j.joca.2020.02.029
24. Bonnevie ED, Delco ML, Bartell LR, et al. Microscale frictional strains determine chondrocyte fate in loaded cartilage. *J Biomech*. 2018;74:72-78.
25. Ayala S, Fortier LA, Delco ML, et al Cartilage articulation enhances chondrocyte injury and death after impact injury. *J Orthop Res*. 2020;28(December):S192-S193. https://pubmed.ncbi.nlm.nih.gov/33274781/
26. Bartell LR, Xu MC, Bonassar LJ, Cohen I. Local and global measurements show that damage initiation in articular cartilage is inhibited by the surface layer and has significant rate dependence. *J Biomech*. 2018;72:63-70.
27. Jay GD, Cha CJ. The effect of phospholipase digestion upon the boundary lubricating ability of synovial fluid. *J Rheumatol*. 1999;26(11):2454-2457.
28. Bonnevie ED, Galesso D, Secchieri C, Cohen I, Bonassar LJ. Elastoviscous transitions of articular cartilage reveal a mechanism of synergy between lubricin and hyaluronic acid. *PLoS One*. 2015;10(11):e0143415.
29. Linn FC. *Lubrication of Animal Joints II the Mechanism**. Pergamon Press; 1968:193-205.
30. Jay GD, Torres JR, Warman ML, Laderer MC, Breuer KS. The role of lubricin in the mechanical behavior of synovial fluid. *Proc Natl Acad Sci*. 2007;104(15):6194-6199. www.pnas.orgcgidoi10.1073pnas.0608558104
31. Bonnevie ED, Delco ML, Fortier LA, Alexander PG, Tuan RS, Bonassar LJ. Characterization of tissue response to impact loads delivered using a hand-held instrument for studying articular cartilage injury. *Cartilage*. 2015;6(4):226-232.
32. Noyes FR, Grood ES. The strength of the anterior cruciate ligament in humans and rhesus monkeys: age related and species related changes. *J Bone Joint Surg Series A*. 1976;58(8):1074-1082.
33. Bonnevie ED, Delco ML, Galesso D, Secchieri C, Fortier LA, Bonassar LJ. Sub-critical impact inhibits the lubricating mechanisms of articular cartilage. *J Biomech*. 2017;53:64-70.
34. Gleghorn JP, Jones ARC, Flannery CR, Bonassar LJ. Boundary mode lubrication of articular cartilage by recombinant human lubricin. *J Orthop Res*. 2009;27(6):771-777.
35. Gleghorn JP, Bonassar LJ. Lubrication mode analysis of articular cartilage using Stribeck surfaces. *J Biomech*. 2008;41(9):1910-1918.
36. Bonnevie ED, Puetzer JL, Bonassar LJ. Enhanced boundary lubrication properties of engineered menisci by lubricin localization with insulin-like growth factor I treatment. *J Biomech*. 2014;47(9):2183-2188.
37. Buckley MR, Gleghorn JP, Bonassar LJ, Cohen I. Mapping the depth dependence of shear properties in articular cartilage. *J Biomech*. 2008;41(11):2430-2437.
38. Middendorf JM, Griffin DJ, Shortkroff S, et al. Mechanical properties and structure-function relationships of human chondrocyte-seeded cartilage constructs after in vitro culture. *J Orthop Res*. 2017;35(10):2298-2306.
39. Silverberg JL, Dillavou S, Bonassar L, Cohen I. Anatomic variation of depth-dependent mechanical properties in neonatal bovine articular cartilage. *J Orthop Res*. 2013;31(5):686-691.
40. Buckley MR, Bonassar LJ, Cohen I. Localization of viscous behavior and shear energy dissipation in articular cartilage under dynamic shear loading. *J Biomech Eng*. 2013;135(3):1-9.
41. Buckley MR, Bergou AJ, Fouchard J, Bonassar LJ, Cohen I. High-resolution spatial mapping of shear properties in cartilage. *J Biomech*. 2010;43(4):796-800. doi:10.1016/j.jbiomech.2009.10.012
42. Silverberg JL, Barrett AR, Das M, Petersen PB, Bonassar LJ, Cohen I. Structure-function relations and rigidity percolation in the shear properties of articular cartilage. *Biophys J*. 2014;107(7):1721-1730. doi:10.1016/j.bpj.2014.08.011

43. Bartell LR, Fortier LA, Bonassar LJ, Cohen I. Measuring microscale strain fields in articular cartilage during rapid impact reveals thresholds for chondrocyte death and a protective role for the superficial layer. *J Biomech*. 2015;48(12):3440-3446. doi:10.1016/j.jbiomech.2015.05.035
44. Schindelin J, Arganda-Carreras I, Frise E, et al. Fiji: an open-source platform for biological-image analysis. *Nat Methods*. 2012;9: 676-682.
45. Rayahin JE, Buhrman JS, Zhang Y, Koh TJ, Gemeinhart RA. High and low molecular weight hyaluronic acid differentially influence macrophage activation. *ACS Biomater Sci Eng*. 2015;1(7):481-493.
46. McKee CM, Penno MB, Cowman M, et al. Hyaluronan (HA) fragments induce chemokine gene expression in alveolar macrophages. The role of HA size and CD44. *J Clin Invest*. 1996;98(10):2403-2413.
47. Euppayo T, Siengdee P, Buddhachat K, et al. Effects of low molecular weight hyaluronan combined with carprofen on canine osteoarthritis articular chondrocytes and cartilage explants in vitro. *In Vitro Cell Dev Biol Animal*. 2015;51(8):857-865. https://link.springer.com/article/10.1007/s11626-015-9908-9
48. Wang CT, Lin YT, Chiang BL, Lin YH, Hou SM. High molecular weight hyaluronic acid down-regulates the gene expression of osteoarthritis-associated cytokines and enzymes in fibroblast-like synoviocytes from patients with early osteoarthritis. *Osteoarthritis Cartilage*. 2006;14(12):1237-1247. https://pubmed.ncbi.nlm.nih.gov/16806998/
49. Elsaid KA, Zhang L, Waller K, et al. The impact of forced joint exercise on lubricin biosynthesis from articular cartilage following ACL transection and intra-articular lubricin's effect in exercised joints following ACL transection. *Osteoarthritis Cartilage*. 2012;20(8):940-948.
50. Jay GD, Waller KA. The biology of lubricin: near frictionless joint motion. *Matrix Biol*. 2014;39:17-24.
51. Jones A, Flannery C. Bioregulation of lubricin expression by growth factors and cytokines. *Eur Cells Mater*. 2007;13:40-45.
52. Lee W, Nims RJ, Savadipour A, et al. Inflammatory signaling sensitizes Piezo1 mechanotransduction in articular chondrocytes as a pathogenic feed-forward mechanism in osteoarthritis. *Proc Natl Acad Sci*. 2021;118(13):e2001611118.https://www.pnas.org/doi/abs/10.1073/pnas.2001611118
53. Zhao Z, Li Y, Wang M, Zhao S, Zhao Z, Fang J. Mechanotransduction pathways in the regulation of cartilage chondrocyte homoeostasis. *J Cell Mol Med*. 2020;24(10):5408-5419.
54. Collins JA, Moots RJ, Winstanley R, Clegg PD, Milner PI. Oxygen and ph-sensitivity of human osteoarthritic chondrocytes in 3-D alginate bead culture system. *Osteoarthritis Cartilage*. 2013;21(11): 1790-1798.
55. Anderson DD, Chubinskaya S, Guilak F, et al. Post-traumatic osteoarthritis: improved understanding and opportunities for early intervention. *J Orthop Res*. 2011;29(6):802-809. https://onlinelibrary.wiley.com/doi/full/10.1002/jor.21359
56. Woodell-May JE, Sommerfeld SD. Role of inflammation and the immune system in the progression of osteoarthritis. *J Orthop Res*. 2020;38(2):253-257. https://onlinelibrary.wiley.com/doi/full/10.1002/jor.24457
57. Whittaker JL, Woodhouse LJ, Nettel-Aguirre A, Emery CA. Outcomes associated with early post-traumatic osteoarthritis and other negative health consequences 3-10 years following knee joint injury in youth sport. *Osteoarthritis Cartilage*. 2015;23(7):1122-1129. doi:10.1016/j.joca.2015.02.021
58. Lieberthal J, Sambamurthy N, Scanzello CR. Inflammation in joint injury and post-traumatic osteoarthritis. *Osteoarthritis Cartilage*. 2015;23(11):1825-1834.
59. Khella CM, Asgarian R, Horvath JM, Rolauffs B, Hart ML. An evidence-based systematic review of human knee post-traumatic osteoarthritis (PTOA): timeline of clinical presentation and disease markers, comparison of knee joint PTOA models and early disease implications. *Int J Mol Sci*. 2021;22(4):1996.
60. Watt FE, Paterson E, Freidin A, et al. Acute molecular changes in synovial fluid following human knee injury: association with early clinical outcomes. *Arthritis Rheum*. 2016;68(9):2129-2140. https://pubmed.ncbi.nlm.nih.gov/26991527/
61. Lopa S, Leijs MJC, Moretti M, Lubberts E, van Osch GJVM, Bastiaansen-Jenniskens YM. Arthritic and non-arthritic synovial fluids modulate IL10 and IL1RA gene expression in differentially activated primary human monocytes. *Osteoarthritis Cartilage*. 2015;23(11):1853-1857. http://www.oarsijournal.com/article/S1063458415012078/fulltext

SUPPORTING INFORMATION

Additional supporting information can be found online in the Supporting Information section at the end of this article.

How to cite this article: Ayala S, Matan SO, Delco ML, Fortier LA, Cohen I, Bonassar LJ. Degradation of lubricating molecules in synovial fluid alters chondrocyte sensitivity to shear strain. *J Orthop Res*. 2024;1-13. doi:10.1002/jor.25960